Trees (2018) 32:1347–1356
https://doi.org/10.1007/s00468-018-1716-x

ORIGINAL ARTICLE

Automatic image processing morphometric method for the analysis of tracheid double wall thickness tested on juvenile *Picea omorika* trees exposed to static bending

Aleksander Nedzved[1] · Aleksandra Lj. Mitrović[2] · Aleksandar Savić[2,3] · Dragosav Mutavdžić[2] · Jasna Simonović Radosavljević[2] · Jelena Bogdanović Pristov[2] · Gabor Steinbach[4,5] · Győző Garab[4] · Valery Starovoytov[1] · Ksenija Radotić[2]

Received: 11 January 2018 / Accepted: 4 June 2018 / Published online: 12 June 2018

Abstract

Key message **We present and test an automatic image processing morphometric method for the analysis of tracheid double wall thickness.**

Abstract Measurements of various anatomical characteristics of wood cells are of great importance in research of wood structure, either for the evaluation of environmental influences or for estimation of wood quality. We present and test an automatic image processing morphometric method for the analysis of tracheid double wall thickness. A new algorithm of image analysis was developed. It uses morphological processing of structural elements with the different orientations from distance maps to analyze tracheid double wall thickness distribution separately for radial walls, tangential walls, and cell corners. For testing the performance of the method, we used confocal laser scanning microscopy images of stem cross-sections of juvenile *Picea omorika* trees exposed to long-term static bending. As a response to mechanical stress, conifers form compression wood (CW), which occurs in a range of gradations from near normal wood (NW) to severe CW. However, visual detection of compression wood severity, more precisely the determination of mild CW, is difficult. One of the anatomic features that characterize CW is increased wall thickness. After testing proposed automatic image processing morphometric method for the analysis of tracheid double wall thickness separately for radial walls, tangential walls and cell corners, combined with statistical analysis, we could suggest it as a tool for estimation of compression wood severity, or for estimation and gradation of changes in tracheid cell wall thickness as a response to environmental influences during growth and developmental process.

Keywords Compression wood · Distance map · Image analysis · *Picea omorika* · Tracheid double wall thickness

Communicated by Y. Sano.

✉ Aleksander Nedzved
Nedzveda@tut.by

✉ Aleksandra Lj. Mitrović
mita@imsi.rs

[1] United Institute of Informatics Problems, Surganova 6, Minsk, Belarus

[2] Institute for Multidisciplinary Research, University of Belgrade, Kneza Višeslava 1, Belgrade 11000, Serbia

[3] Laboratoire de Spectrochimie Infrarouge et Raman-UMR 8516, Université de Lille, Sciences et Technologies, 59655 Villeneuve d'Ascq Cedex, France

[4] Institute of Plant Biology, Biological Research Center, Szeged 6701, Hungary

[5] Institute of Microbiology, CAS, Centrum Algatech, Třeboň, Czech Republic

Introduction

Wood properties are directly determined by cell arrangement, cell size and shape, and cell wall structure and thickness. Each species is characterized by a relatively constant arrangement of tissue elements, which is thus in use for wood species identification (Smith 1967). On the other hand, differences in macroscopic and microscopic structure of wood in softwood species result from genetic and abiotic factors: plant age (juvenile or mature wood—Zobel and Sprague 1998; Plomion et al. 2001), season of maturation within the growth ring (early and late wood—Uggla et al. 2001) or mechanical stress as a consequence of wind and stem lean (compression wood, opposite wood and normal wood—Timell 1986). In the forest products' industry, juvenile wood, early wood and compression wood, generally

have limited value, and therefore the determination of their amounts is of great importance. Cross-sectional tracheid shapes are a good indicator of the anisotropy of wood properties (Watanabe et al. 1998), thus measurements of various cross-sectional dimensions of wood cells are often used in comparative research of wood structure, either for evaluating environmental influences, or for structure/properties ratio estimation as important features that distinguish wood quality. Different methods have been applied for measuring different wood cell dimensions (cell wall area, radial cell wall width, double wall thickness, or cell lumen), such as manual and automated measurements on micrographs (Mork 1928; Brown et al. 1949; Gofas and Tsoumis 1975; Klisz 2009; Selig et al. 2012), or from distance maps reconstructed from digital images (Travis et al. 1996; Lorbach et al. 2012). Such measurements have been widely in use for estimation of early wood (EW) and late wood (LW) ratio within an annual ring in gymnosperms by Mork's index (Mork 1928), circularity index (Jagels and Dyer 1983), or aspect ratio (Diao et al. 1999).

Tracheid double wall thickness, as an important wood anatomical feature, besides being known as an indicator of transition from EW to LW within an annual ring in gymnosperms (the ratio between radial double cell wall thickness and cell lumen diameter, Mork 1928), also characterizes the differences between juvenile and mature wood (Mitchell and Denne 1997; Luostarinen 2012), as well as between normal and compression wood (Timell 1986; Plomion et al. 2001). Hence, determination of tracheid double wall thickness could provide good evidence of environmental influences during conifer trees growth and development.

In this study, we present and test an automatic image processing morphometric method for the analysis of tracheid double wall thickness. The use of Euclidian distance maps for calculating the thickness of wood cell wall was suggested earlier in estimations of pulp or paper quality (Koskenhely and Paulapuro 2005; Selig et al. 2012; Lorbach et al. 2012). The novelty of our method is the use of morphological image processing of structural elements with the different orientations (Dougherty 1992) on Euclidian distance maps reconstructed from microscopic images. This kind of image processing allows determination of the distribution of tracheid double wall thickness separately for tangential walls, radial walls, and cell corners.

For testing the performance of our automatic image processing morphometric method, we used confocal laser scanning microscopy (CLSM) images of stem cross-sections of juvenile *P. omorika* trees exposed to long-term static bending. Conifers, as a response to mechanical stress, form reaction wood called compression wood (CW) (Timell 1986). Compression wood occurs in a range of gradations from near normal wood (NW) to severe CW (SCW), mild CW (MCW) forming a continuum between NW and severe CW. In slow-growing natural conifer trees, CW, if present, typically occurs in a severe form, but in fast growing plantation forests and in juvenile wood, a mild form of CW can often be found (Donaldson et al. 2004). Conifer young trees, both in virgin forests of spruce and in pine plantations, contain a fair amount of CW, being usually most evident near the pith, as a young thin stem frequently needs to reorient itself, by constant lean corrections under the influence of wind, or by reposition of its crown to better capture the light (Timell 1986). Under the influence of constant wind with changing direction, CW may form around the entire growth ring even in straight vertical fast growing young conifer stems (Barnett et al. 2014). Compression wood formed under moderate wind conditions was found to be MCW (Donaldson and Singh 2013). Correspondingly, artificial inclination at the small angle of juvenile *Picea glauca* trees resulted in MCW formation, while inclination at the high angle resulted in SCW formation (Yumoto et al. 1983). Anatomic features of severe CW includes: increased wall thickness, reduced lumen diameter, rounder cell cross-sectional profile, presence of intercellular spaces, S2 layer divided into an outer S2L region and an inner S2 region containing helical cavities, and absence of S3 layer (Yumoto et al. 1983; Plomion et al. 2001; Donaldson et al. 2004). Mild CW tracheids may have a distinct S3 layer; they show the varying extent of development of S2L region, no helical cavities, thicker cell walls than the NW and lack of intercellular spaces (Yumoto et al. 1983; Donaldson et al. 1999; Donaldson and Singh 2013). The degree of development of particular features of CW does not necessarily change in parallel to each other, so the severity of a given tracheid is represented as a function of the degrees of development of individual features, mainly lignification, helical cavities and cell wall thickness (Yumoto et al. 1983). Although cell wall thickness is strongly subjected to the annual variation, with some limitations it could be an indicator of CW severity (Yumoto et al. 1983). As the severity of compression wood affects mechanical and chemical properties of wood, it is desirable to be able to measure CW severity (Altaner et al. 2009). Since visual detection of compression wood severity, more precisely the determination of mild CW, is difficult, different digital image analysis techniques for distinguishing wood samples on a compression severity scale were developed (Andersson and Walter 1995; Nyström and Hagman 1999; Moëll and Fujita 2004; Duncker and Spiecker 2009; Savić et al. 2016).

Various non-morphometric methods for quantification of compression wood severity based on lignin content and structure, as the most reliable indicator of compression wood, and polysaccharides composition and organization, have also been established: scanning Fourier transform infrared microspectroscopy and immunolabeling of

(1–4)-β-galactan (Altaner et al. 2009), chemical analysis (Nanayakkara et al. 2009), fluorescence spectroscopy and spectral analysis of lignin (Donaldson et al. 2010).

Our automatic image processing morphometric method that enables the assessment of double cell wall thickness, separately for different regions of tracheid cell wall (radial, tangential, and cell corners), could provide valuable data in evaluation of environmental influences during conifer trees growth and development, and consequently in estimation of wood quality, as wood properties are directly determined, among other features, by tracheid wall shape and thickness.

Materials and methods

Plant growth and sample collection

Picea omorika (Pančić) Purkyně, the Serbian spruce, is a Balkan endemic coniferous species and tertiary relict of the European flora. Despite its endemism, *P. omorika* is considered as one of the most adaptable spruces. It belongs to slow-growing conifer species, its wood is characterized by small, densely packed tracheids, while CW typically occurs in a severe form (Timell 1986; Donaldson et al. 2004).

Four-year-old *P. omorika* trees were grown in plastic pots (20 × 20 × 20 cm) outdoors in Belgrade, Serbia (44°49′N, 20°29′E). The plants were about 70 cm tall. Severe static bending stress was applied by wiring at the end of the growing season, in October 2009. The bending angle was about 90° (Mitrović et al. 2015). Stem samples (about 3 cm long) were taken at about 15 cm from the stem base in July 2010, and then debarked, air dried, and 100 µm thick cross-sections were prepared on a microtome.

Selection of CW wood samples for microscopic analysis was made by location relative to stem bending. Strongly leaned trees form SCW on the lower side of the lean, while on the lateral sides form MCW (Yumoto et al. 1983). So, SCW samples (S5 and S6, Fig. 1) were selected from the lower side of the lean, while MCW samples were selected from the lateral sides (S3 and S4, Fig. 1) of the last growth ring from plants exposed to long-term static bending. Normal wood is often uncommon in juvenile conifers, as they produce large amounts of randomly distributed mild CW (Donaldson et al. 2004). So, NW samples (S1 and S2, Fig. 1) were selected from the growth ring with the lowest amount of CW.

Confocal microscopy

Cross-sections, 100 µm thick, of air-dried stem samples were stained for two hours in Congo Red 1 mM solution (from Sigma, Steinheim, Germany) and then washed with deionised water to remove the unbound dye.

For imaging, we used a Zeiss LSM 410 microscope. Confocal images were 512 × 512 pixels, with 160 × 160 µm image physical size and 0.3125 µm pixel size, using a 40×/0.75 objective and 2× zoom (Fig. 1). Congo Red was excited using the 488 nm line of the Ar-ion laser, and fluorescence emission was detected above 560 nm. Analyzed stem cross-sections were always oriented the same way—tracheid tangential walls parallel to the *X*-axis and radial walls parallel to the *Y*-axis, to be able to determine tangential and radial double wall thickness.

Tracheid cell wall analysis on digital images

A new algorithm for image analysis was developed for calculating double cell wall thickness. This algorithm was realized in the universal system for image analysis—Imagewarp (http://www.imagewarp.com/) from A&B Software company (USA). It is realized as specific scripts that use the function of Imagewarp such as distance map, gray-scale thinning, mathematical morphology and measurement. Also, these scripts were adapted for software for image analysis QTIP that was developed in United Institute of Informatics Problems (UIIP), National Academy of Sciences (Belarus). The first step of this algorithm is the extraction of cell patterns on the original image. It was performed via binarization (Fig. 1) of the enhanced image using Otsu's threshold method (Otsu 1979). The result is an aligned histogram of brightness and the threshold for binarization is selected on it. The threshold is unique for each image. This way the shading of the confocal images due to a change in the depth of the focal plane is overcome to a significant extent. After that, operations of mathematical morphology were applied to the binary images (Fig. 1) for their shape correction. The next step is the reconstruction of the distance maps (Kimmel et al. 1996) obtained from the images (Fig. 1) to determine the distances between lumens of two adjacent cells.

The intensity of each pixel on the distance map image corresponds to the distance to the nearest cell lumen. The distance between lumens of two adjacent cells was determined as a conjunction of the morphological medial lines and the distance map. To find the morphological medial lines, pixels corresponding to the local maxima were found and then gray thinning was applied to those pixels (Ablameyko et al. 2006).

For the construction of a distance map, a gray-scale image is represented as 3D shape (Fig. 2a) or as a collection of binary layers where every lower layer includes pixels from a higher layer. The 3D space is represented in horizontal, vertical and brightness axis (Fig. 2a, c). This way the image is described as a topological surface. Distance map of one binary layer is constructed by increasing pixels depth for reflecting distance properties of pixels. A gray-scale image has up to 256 Gy levels. In this way, a binary image may

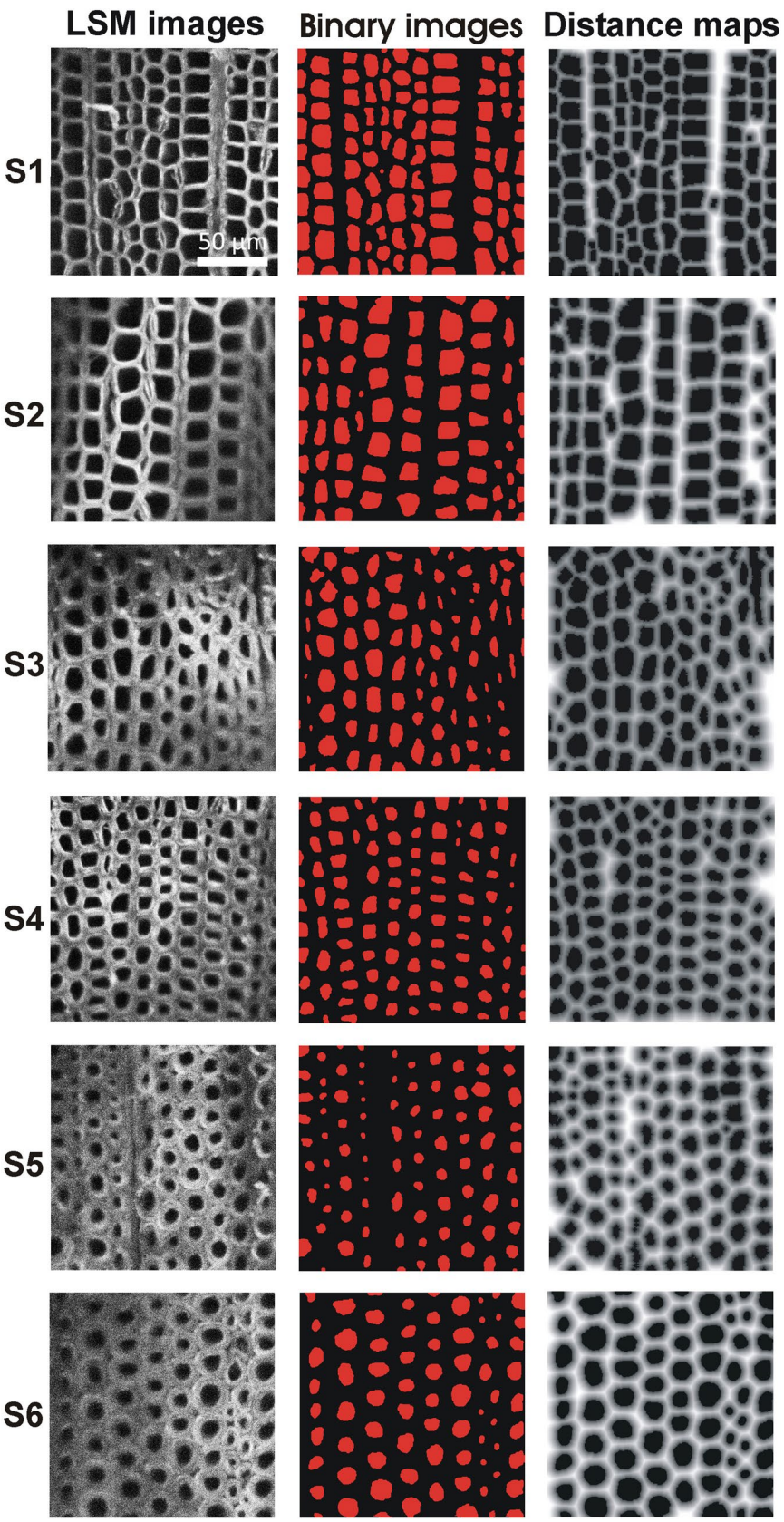

Fig. 1 The CLSM images (first column, image size 512×512 pixels, with 160×160 µm image physical size and 0.3125 µm pixel size), corresponding binary images (second column) and distance maps (third column) of *P. omorika* stem samples; S1 and S2—NW samples, selected from the growth ring with the lowest amount of CW; S3 and S4—MCW samples, selected from the lateral sides of the last growth ring from plants exposed to long-term static bending; S5 and S6—SCW samples, selected from the lower side of the lean of the last growth ring from plants exposed to long-term static bending; number of analysed tracheids per sample: 93 (S1), 53 (S2), 75 (S3), 99 (S4), 80 (S5), 62 (S6)

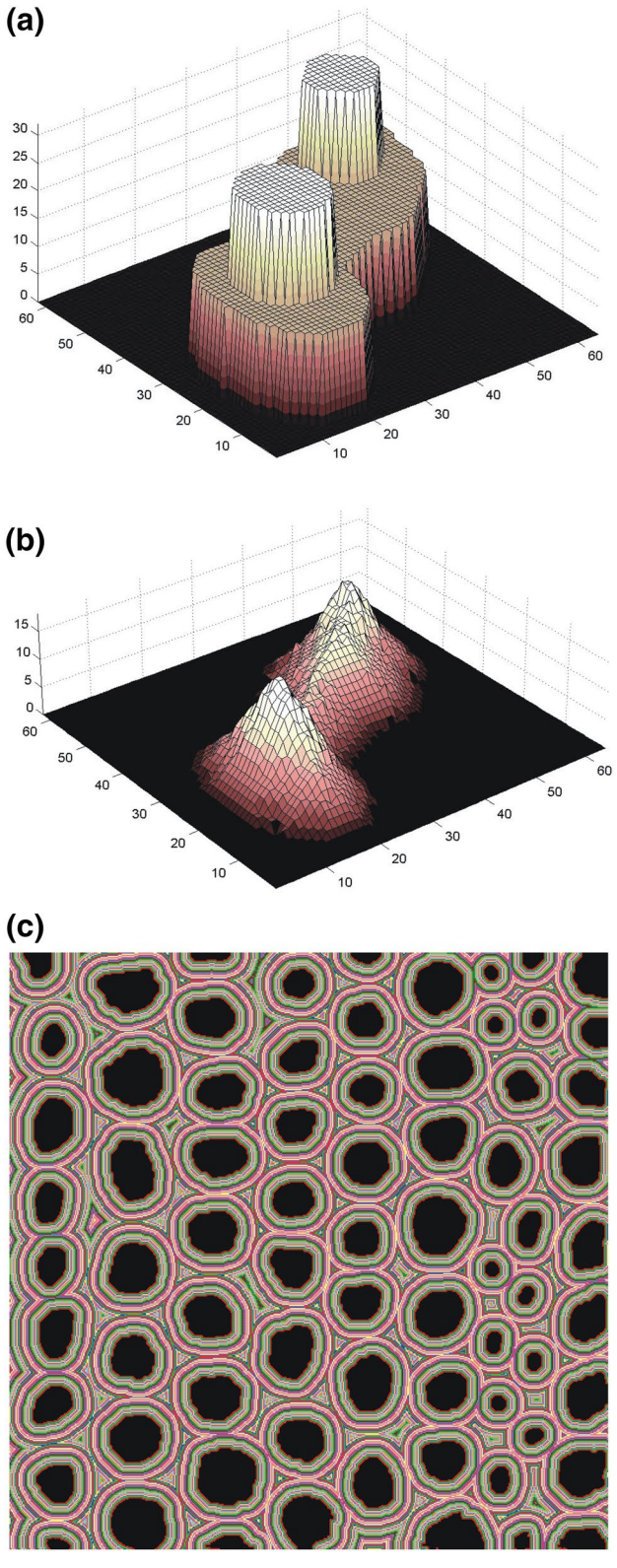

Fig. 2 Construction of a distance map: **a** example of an object as the 3D representation of the image as topological surface, the 3D space is represented by *X*-, *Y*-, and brightness axis (*Z*-axis), **b** its distance map; **c** distance map (2D) that corresponds to S6 sample from Fig. 1

be constructed as the cross-section of the two-dimensional brightness function of the gray-scale image, and one may construct up to 255 binary images.

Our algorithm of the distance transform contains two raster-scans of the image. The first scan is realized in the direction from top to bottom of the original gray-scale image and then from left to right. For constructing pseudo-distance maps in this direction, every pixel is changed by the following condition:

$$p = \begin{cases} (p_i + f_i), & \text{if} \quad (p_i + f_i < p) \text{ and } (p_i + f_i \geqslant L(p)) \ , \ i = 0, ..., n \\ L(p), & \text{if} \quad (p_i + f_i < L(p)) \ , \ i = 0, ..., n \\ p, & \text{another case} \end{cases},$$

where p—is the pixel gray value, $L(p)$—the level of a binary layer in the image, p_i—the value of neighborhood pixels, f_i—the value of the corresponding point from the mask-table for Chamfer metrics (Fig. 2), i—index of the element in the mask-table, n—number of elements in mask-table. The second scan is realized by the similar condition with direction from bottom to top and from right to left. It finalizes construction of the distance map for every binary layer. In result, we have a set of layers of distance maps for all layers. Every layer starts from a fixed value, which is multiplied by 256. In the result, numbers of the map reflect combined properties of the pixel gray-values and distances. Example of the distance map is shown in Fig. 2c.

Using the calculated distance map, one can use a thinning algorithm that is based on the metric used for the distance map construction. The algorithm for detection of skeleton pixels consists of two parts (see Table 1):

1. Detection of feature pixels (topological properties):

a. End pixels;
b. Saddle pixels;
c. Duplex of saddle pixels;
d. Local maximum.

2. Determination of remaining elements of a skeleton.

Example of the gray-level skeleton is shown in Fig. 2c.

The result of distance map thinning is the skeleton of all double walls on the image that consist of ridge pixels from the distance map. For this skeleton, the distribution of pixel brightness corresponds to the distribution of double wall thickness in pixels.

The next step in our new algorithm was the classification of resulting lines (Fig. 3) by orientation to determine double wall thickness of radial and tangential walls (Fig. 3c, d). It

Table 1 Conditions to detect feature pixels

End pixels (p)	$\Sigma(p_i \geq p) > 0$
Saddle pixels	(c_4 and c_0 and not c_2 and not c_6) or (not c_4 and not c_0 and c_2 and c_6) or [c_1 and c_5 and not (c_2 and c_3 and c_4) and not (c_0 and c_7 and c_6)] or [c_3 and c_7 and not (c_2 and c_1 and c_0) and not (c_4 and c_5 and c_6)]
Duplex of saddle pixels (two pixels p and p_i, when i—neighbor, that is tested by FindMax function)	(c_5 and $n_1 = p$ and not c_0 and not c_2) and FindMax(1) > 0 (c_1 and $n_5 = p$ and not c_6 and not c_4) and FindMax(5) > 0 (c_3 and $n_7 = p$ and not c_0 and not c_6) and FindMax(7) > 0 (c_7 and $n_3 = p$ and not c_2 and not c_4) and FindMax(3) > 0 (c_4 and $n_0 = p$ and not c_2 and not c_6) and FindMax(0) > 0 (c_0 and $n_4 = p$ and not c_2 and not c_6) and FindMax(4) > 0 (c_6 and $n_2 = p$ and not c_4 and not c_0) and FindMax(2) > 0 (c_2 and $n_6 = p$ and not c_4 and not c_0) and FindMax(6) > 0
Local maximum	$\Sigma(p_i > p) = 0$

Where p—a current pixel, p_i—neighbor, c_i–condition ($p_i > p$), and, or, not—logical operators: conjunction, disjunction, negation, FindMax(i)—function for the count of pixels with greater level from neighborhood i: $\text{FindMax}(i) = \sum_{j=0}^{n} \begin{cases} 1, & if(p_i < p_{i,j}) \\ 0, & \text{in otherwise} \end{cases}$, where $p_{i,j}$—neighbor of p_i.

is realized by morphological processing with structure elements of different orientation (Dougherty 1992). As a result we calculated: distribution of double wall thickness of entire tracheids (Fig. 3a), distribution of double wall thickness of tracheids at cell corners (Fig. 3b, which yields information on circularity/rectangularity of cross-sectional profile of tracheid wall), and distribution of double wall thickness of radial and tangential walls (Fig. 3d).

To the obtained set of data (the distribution of pixel brightness which corresponds to distribution of double wall thickness in pixels), we applied IBM SPSS software, Nonlinear Curve Fit function for fitting the Gaussian curves on the data that were used to show the overall variation in tracheid double cell wall thickness in a response to mechanical stress. For comparison of the maxima positions of Gaussian curves between samples S1–S6 (Fig. 1), we used one-way ANOVA to test for significant differences, while the Duncan test was used for post hoc analysis. In all tests, $p \leq 0.05$ was used to define "significant difference".

Results and discussion

Image processing techniques are in use for estimation of the EW and LW ratio as a significant feature for forest products' industry (Mork 1928; Jagels and Dyer 1983; Diao et al. 1999). Computerized image analysis has also been suggested as a tool for estimation of pulp or paper quality (Koskenhely and Paulapuro 2005; Selig et al. 2012; Lorbach et al. 2012) The efforts to use such techniques for the estimation of compression wood severity were more (Duncker and Spiecker 2009; Savić et al. 2016) or less (Andersson and Walter 1995; Nyström and Hagman 1999; Moëll and Fujita 2004) successful in recognizing mild CW.

Here we present and test an automatic image processing morphometric method for the analysis of tracheid double wall thickness. Our new algorithm consists of the extraction of cell patterns from the original microscopy image via binarization using Otsu's threshold method (Otsu 1979) and reconstruction of the distance maps (Kimmel et al. 1996). The use of Euclidian distance maps for calculating the thickness of wood cell wall was suggested earlier in estimations of pulp or paper quality (Travis et al. 1996; Koskenhely and Paulapuro 2005; Selig et al. 2012; Lorbach et al. 2012). The novelty of our method is the use of morphological image processing of structural elements with the different orientations (Dougherty 1992) on distance maps reconstructed from microscopic images, allowing determination of the distribution of tracheid double wall thickness separately for tangential walls, radial walls, and cell corners (Fig. 4b–d).

We test our automatic image processing morphometric method using CLSM images of stem cross-sections of juvenile *P. omorika* trees exposed to long-term static bending. As samples for the analysis were selected from the last growth ring from plants exposed to static bending, as well as from the growth ring with the lowest amount of CW (S1 and S2), this is at the same time the test of our method as a tool for

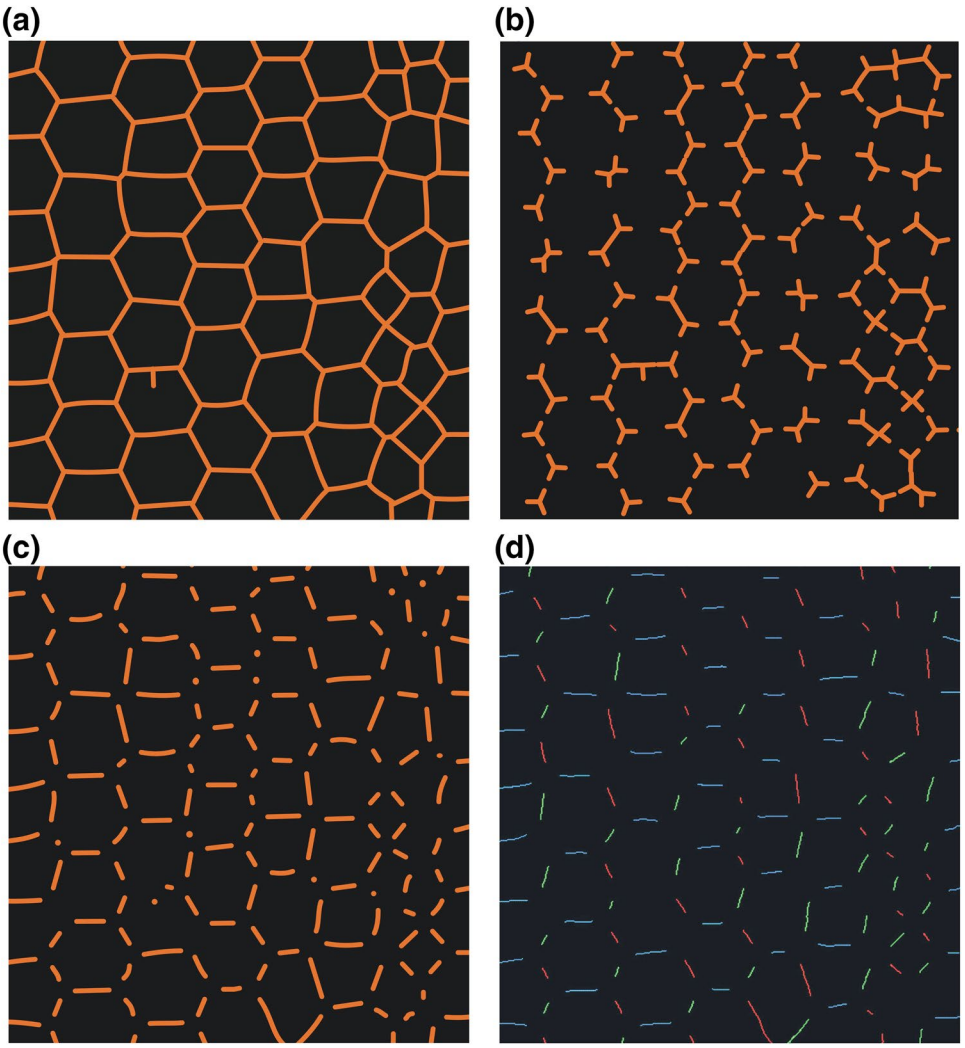

Fig. 3 The result of thinning of distance map: **a** skeleton of all double cell walls; **b**–**d** topological features of cell walls: **b** fragments of double cell walls skeleton (nodes in the skeleton) representing cell walls at cell corners; **c** fragments of double cell walls, separated as branches of the wall skeleton; **d** classification of those fragments by orientation (green and red lines—radial walls; blue lines—tangential walls)

estimation of compression wood severity. Juvenile conifer stem samples could be a good choice of samples for evaluating the precision of methods for estimation of compression wood severity, since juvenile conifers produce randomly distributed MCW (Donaldson et al. 2004). The examples are the methods successful in the estimation of compression wood severity, which were evaluated on samples of juvenile *Picea abies* (Duncker and Spiecker 2009) and *P. omorika* (Savić et al. 2016).

One-way ANOVA and Duncan test were performed for the maxima positions of Gaussian curves of the distribution of pixel brightness corresponding to double wall thickness distribution for the samples S1–S6 (Fig. 1). As a result, our image processing method aligns juvenile *P. omorika* wood samples from NW to severe CW (Fig. 4a–d), suggesting that it could be used as a tool for fine gradation of wood samples on compression severity scale. On the obtained scales (Fig. 4a–d), the samples S1 and S2 (Fig. 1), representatives of NW, selected from the growth ring with the lowest amount of CW, are positioned to the left. The samples S5 and S6, representatives of SCW, selected from the lower side of the last growth ring from plants exposed to long-term static bending, are positioned to the right (Fig. 4a–d). The samples S3 and S4, representatives of MCW, selected from the lateral sides of the last growth ring from plants exposed to static bending, are positioned in the middle of the formed scale (Fig. 4a–d).

In addition, our automatic image processing morphometric method separates samples S1 and S2 (Fig. 1), representatives of NW, positioning the S2 sample to the right on the scale, closer to mild compression wood samples S3 or S4 (Fig. 4a–d). This could be easily explained as NW samples (S1 and S2) were selected from the growth ring with the lowest amount of CW, since juvenile conifers produce large amounts of randomly distributed mild CW, NW often being uncommon (Donaldson et al. 2004).

However, compression severity scales based on double wall thickness distribution of entire tracheids (Fig. 4a), tracheids at cell corners (Fig. 4b), tangential (Fig. 4c) and radial walls (Fig. 4d), differ to some degree. Compression severity

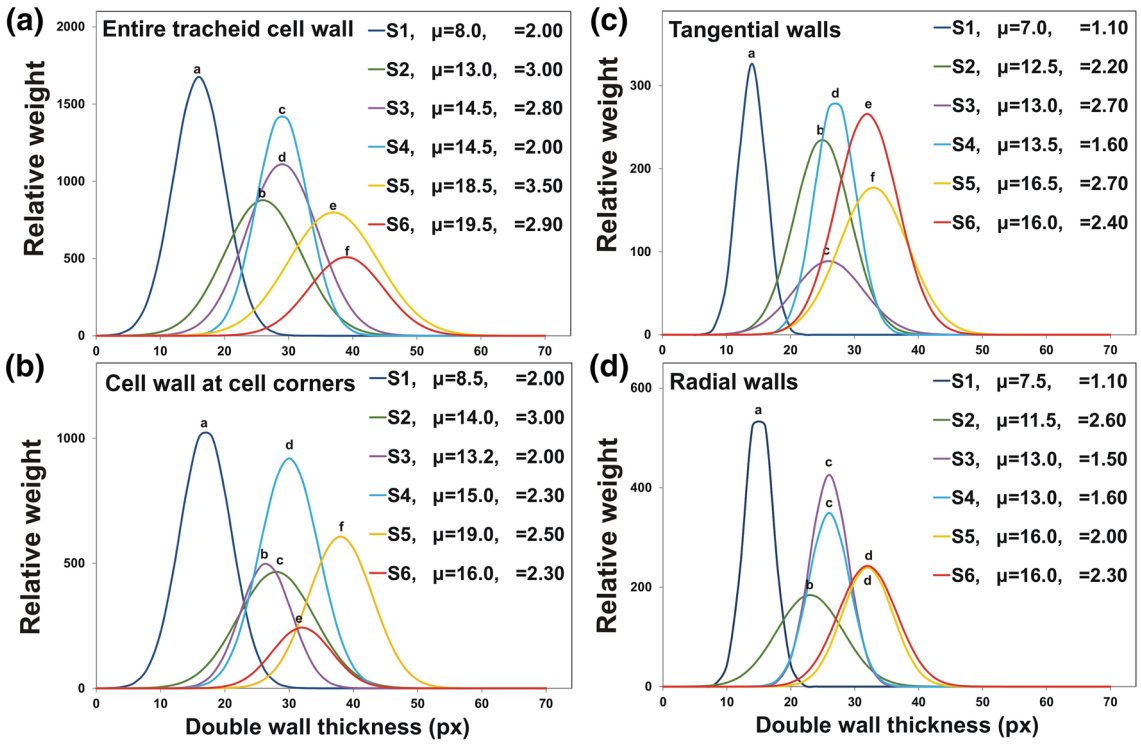

Fig. 4 Distribution of double wall thickness of **a** entire tracheid walls, **b** tracheid at cell corners, **c** tangential walls and **d** radial walls, determined by morphological processing of structural elements with different orientation from distance maps obtained from the CLSM images of (S1–S6) samples (Fig. 1); **a**–**f** significant difference at 5% level of significance of the maxima positions of Gaussian curves between samples S1–S6 from Fig. 1; μ mean values, σ standard deviation, *px* pixels

scale based on double wall thickness distribution of entire tracheids (Fig. 4a) aligns samples (S1-S6, Fig. 1) in the following order: S1, S2, S4, S3, S5, S6; the scale based on double wall thickness distribution of tracheids at cell corners (Fig. 4b): S1, S3, S2, S4, S6, S5; the scale based on double wall thickness distribution of tangential walls (Fig. 4c): S1, S2, S3, S4, S6, S5. This suggests that different regions of *P. omorika* tracheid cell wall (radial walls, tangential walls, and cell corners) show somewhat different cell wall thickening in response to mechanical stress.

Compression severity scale based on double wall thickness distribution of radial walls (Fig. 4d) shows additional specificity: there is no significant difference between maxima positions of Gaussian curves for the samples S3, S4, and S5, S6, respectively. In other words, compression severity scale based on double wall thickness distribution of radial walls (Fig. 4d) is grouping, and consequently sharply distinguishing mild CW samples (S3 and S4) from severe CW samples (S5 and S6).

It is known that radial and tangential walls can vary significantly regarding cellulose microfibril angle as the most commonly measured feature of wood cell walls (Gorišek and Torelli 1999; Khalili et al. 2001; Anagnost et al. 2005), or regarding distribution and order of cellulose fibrils (Savić et al. 2016). So far, most investigations, regarding cellulose microfibrils (Donaldson 2008), or other features of wood cell walls such as cell wall thickness (Mork 1928), have been carried out on radial cell walls.

After testing our automatic image processing morphometric method for the analysis of tracheid double cell wall thickness, combined with statistical analysis, on wood samples of juvenile *P. omorika* exposed to long-term static bending, we could suggest it as a tool for fine gradation of conifer wood samples on a compression severity scale.

Conclusion

We have presented hereby an automatic image processing morphometric method for the analysis of tracheid double wall thickness. We have tested the performance of our method on CLSM images of stem cross-sections of juvenile *P. omorika* trees exposed to long-term static bending. The method has many advantages with a small number of requirements. It enables fast automatic analyses of wood samples. It is independent of the type of microscopy used. The quality of digital images is not limiting, as only the contrast between cell lumen and cell wall is of interest. The only

requirement concerning image quality is the use of microscopic images of the same resolution. Our method applies a new algorithm of image analysis to examine double wall thickness distribution of radial walls, tangential walls and cell corners separately, based on the morphological processing of structural elements with the different orientation from distance maps. That is the reason for the second requirement of our method—tangential and radial walls must be oriented the same way on all microscopic images being compared.

We showed that our morphometric method analyzing double wall thickness distribution of entire tracheids, tracheids at cell corners, tangential and radial walls, provides a fine gradation of juvenile *P. omorika* wood samples from NW to the severest form of CW, compression severity scales being partially different. Radial walls double wall thickness distribution, in addition, is grouping and consequently sharply distinguishing mild CW samples from severe CW samples, and hence could be suggested as a useful and rapid tool for distinguishing severe CW samples from mild CW samples. The presented result could qualify our method for use in estimation of compression wood severity in forest products industries, alone or in combination with other non-morphometric methods.

Our new image processing algorithm, combined with statistical analysis, could be a useful tool in estimation and gradation of changes in tracheid cell wall thickness as a response to environmental influences during growth and developmental process. As tracheid radial and tangential walls can vary significantly regarding cell wall thickness, its potential for estimation of double wall thickness distribution separately for different regions of tracheid cell wall (radial walls, tangential walls, and cell corners) is a valuable advantage of our automatic morphometric method.

Author contribution statement AM, JBP, JSR and KR—experimental design, sample collection and processing. AS, GS and GG—confocal laser scanning microscopy. AN and VS—image processing methods. DM—statistical data analysis. AM, and KR—general consideration of the results and writing the manuscript. KR—coordinated the study.

Acknowledgements This study was supported by Grant 173017 of the Ministry of Education, Science and Technological Development of the Republic of Serbia. It was also funded by the bilateral project "Structural anisotropy of plant cell walls of various origin and their constituent polymers, using differential-polarized laser scanning microscopy (DP-LSM)", of the Republic of Serbia and the Republic of Hungary (Institutions: IMSI, University of Belgrade, Serbia, and Institute of Plant Biology, Biological Research Center, Hungarian Academy of Sciences, Hungary), and the bilateral project "Advanced image analysis on micron scale in biology and medicine" of the Republic of Serbia and the Republic of Belarus (Institutions: IMSI, University of Belgrade, Serbia, and United Institute of Informatics Problems, National Academy of Sciences of Belarus, Minsk, Belarus). The study was also partly funded by the project Algain (EE2.3.30.0059) and institutional projects Algatech (CZ.1.05/2.1.00/03.0110), GINOP-2.3.2-15-2016-00001 and Algatech Plus (MSMT LO1416).

Compliance with ethical standards

Conflict of interest The authors declare that they have no conflict of interest.

References

Ablameyko S, Uchida S, Nedzved A (2006) Gray-scale thinning by using a pseudo-distance map. In: Proc of 18th International conference on pattern recognition ICPR, 20–24 August 2006, Hong Kong, vol. 2, pp 239–242

Altaner CM, Tokareva EN, Wong JC, Hapca AI, McLean JP, Jarvis MC (2009) Measuring compression wood severity in spruce. Wood Sci Technol 43:279–290

Anagnost SE, Mark RE, Hanna RB (2005) S2 orientation of microfibrils in softwood tracheids and hardwood fibres. IAWA J 26:325–338

Andersson C, Walter F (1995) Classification of compression wood using digital image analysis. For Prod J 45:87–92

Barnett J, Gril J, Saranpää P (2014) Introduction. In: Gardiner B, Barnett J, Saranpää P, Gril J (eds) The Biology of Reaction Wood. Springer Series in Wood Science. Springer, Heidelberg, pp 1–11

Brown HP, Panshin AJ, Forsaith CC (1949) Textbook of wood technology. McGraw Hill Book Company Inc, New York

Diao XM, Furuno T, Fujita M (1999) Digital image analysis of cross-sectional tracheid shapes in Japanese softwoods using the circularity index and aspect ratio. J Wood Sci 45:98–105

Donaldson L (2008) Microfibril angle: measurement, variation and relationships—a review. IAWA J 29:345–386

Donaldson LA, Singh AP (2013) Formation and structure of compression wood. In: Fromm J (ed) Cellular aspects of wood formation. Springer, Hamburg, pp 225–256

Donaldson LA, Singh AP, Yoshinaga A, Takabe K (1999) Lignin distribution in mild compression wood of *Pinus radiata*. Can J Bot 77:41–50

Donaldson LA, Grace JC, Downes G (2004) Within tree variation in anatomical properties of compression wood in radiata pine. IAWA J 25:253–271

Donaldson LA, Radotić K, Kalauzi A, Djikanović D, Jeremić M (2010) Quantification of compression wood severity in tracheids of Pinus radiata D. Don using confocal fluorescence imaging and spectral deconvolution. J Struct Biol 169:106–115

Dougherty ER (1992) An introduction to morphological image processing. SPIE Optical Engineering Press, Washington, DC

Duncker P, Spiecker H (2009) Detection and classification of norway spruce compression wood in reflected light by means of hyperspectral image analysis. IAWA J 30:59–70

Gofas A, Tsoumis G (1975) A method for measuring characteristics of wood. Wood Sci Technol 9:145–152

Gorišek Ž, Torelli N (1999) Microfibril angle in juvenile, adult and compression wood of spruce and silver fir. Phyton 39:129–132

Jagels R, Dyer M (1983) Morphometric analysis applied to wood structure. I. Cross-sectional cell shape and area change in red spruce. Wood Fiber Sci 15:376–386

Khalili S, Nilsson T, Daniel G (2001) The use of soft rot fungi for determining the microfibrillar orientation in the S2 layer of pine tracheids. Holz Roh Werkst 58:439–447

Kimmel R, Kiryati N, Bruckstein AM (1996) Distance maps and weighted distance transforms. J Math Imaging Vis Special Issue Topol Geometry Comput Vis 6:223–233

Klisz M (2009) WinCell—an image analysis tool for wood cell measurements. For Res Pap 70:303–306

Koskenhely K, Paulapuro H (2005) Effect of refining intensity on pressure screen fractionated softwood kraft. Nord Pulp Pap Res J 20:169–175

Lorbach C, Hirn U, Kritzinger J, Bauer W (2012) Automated 3D measurement of fiber cross section morphology in handsheets. Nord Pulp Paper Res J 27:264–269

Luostarinen K (2012) Tracheid wall thickness and lumen diameter in different axial and radial locations in cultivated *Larix sibirica* trunks. Silva Fenn 46:707–716

Mitchell MD, Denne MP (1997) Variation in density of *Picea sitchensis* in relation to within-tree trends in tracheid diameter and wall thickness. Forestry 70:47–60

Mitrović A, Donaldson LA, Djikanović D, Bogdanović Pristov J, Simonović J, Mutavdžić D, Kalauzi A, Maksimović V, Nanayakkara B, Radotić K (2015) Analysis of static bending-induced compression wood formation in juvenile *Picea omorika* (Pančić) Purkyně. Trees Struct Funct 5:1533–1543

Moëll MK, Fujita M (2004) Fourier transform methods in image analysis of compression wood at the cellular level. IAWA J 25:311–324

Mork E (1928) Die Qualität des Fichtenholzes unter besonderer Rücksichtnahme auf Schleif—und Papierholz. Der Papier Fabrikant 26:741–747

Nanayakkara B, Manley-Harris M, Suckling ID, Donaldson LA (2009) Quantitative chemical indicators to assess the gradation of compression wood. Holzforschung 63:431–439

Nyström J, Hagman OJ (1999) Real-time spectral classification of compression wood in *Picea abies*. Wood Sci: 45:30–37

Otsu N (1979) A threshold selection method from gray-level histograms. IEEE Trans Syst Man Cybern 9:62–66

Plomion C, Le Provost G, Stokes A (2001) Wood formation in trees. Plant Physiol 127:1513–1523

Savić A, Mitrović A, Donaldson L, Simonović Radosavljević J, Bogdanović Pristov J, Steinbach G, Garab G, Radotić K (2016) Fluorescence-detected linear dichroism of wood cell walls in juvenile Serbian spruce: estimation of compression wood severity. Microsc Microanal 22:361–367

Selig B, Luengo Hendriks CL, Bardage S, Daniel G, Borgefors G (2012) Automatic measurement of compression wood cell attributes in fluorescence microscopy images. J Microsc 246:298–308

Smith DM (1967) Microscopic methods for determining cross-sectional cell dimensions. US For Serv Res Pap FPL 79:20

Timell TE (1986) Compression wood in gymnosperms. Springer, Heidelberg

Travis AJ, Hirst DJ, Chesson A (1996) Automatic classification of plant cells according to tissue type using anatomical features obtained by the distance transform. Ann Bot 78:325–331

Uggla C, Magel E, Moritz T, Sundberg B (2001) Function and dynamics of auxin and carbohydrates during earlywood/latewood transition in Scots pine. Plant Physiol 125:2029–2039

Watanabe U, Norimoto M, Fujita M (1998) Transverse shrinkage anisotropy of coniferous wood investigated by the power spectrum analysis. J Wood Sci 44:9–14

Yumoto M, Ishida S, Fukazawa K (1983) Studies on the formation and structure of compression wood cells induced by artificial inclination in young trees of *Picea glauca*. IV. Gradation of the severity of compression wood tracheids. Res Bull Coll Exp For Hokkaido Univ 40:409–454

Zobel BJ, Sprague JR (1998) Juvenile wood in forest trees. Springer Series in Wood Science, Berlin, p 300